

Theory of fractional-Lévy kinetics for cold atoms diffusing in optical lattices

D. A. Kessler¹ and E. Barkai¹

¹*Department of Physics, Institute of Nanotechnology and Advanced Materials, Bar Ilan University, Ramat-Gan 52900, Israel*

Recently, anomalous superdiffusion of ultra cold ⁸⁷Rb atoms in an optical lattice has been observed along with a fat-tailed, Lévy type, spatial distribution. The anomalous exponents were found to depend on the depth of the optical potential. We find, within the framework of the semiclassical theory of Sisyphus cooling, three distinct phases of the dynamics, as the optical potential depth is lowered: normal diffusion; Lévy diffusion; and $x \sim t^{3/2}$ scaling, the latter related to Obukhov's model (1959) of turbulence. The process can be formulated as a Lévy walk, with strong correlations between the length and duration of the excursions. We derive a fractional diffusion equation describing the atomic cloud, and the corresponding anomalous diffusion coefficient.

PACS numbers: 05.40.Fb, 37.10.Jk

Very recently, Sagi et al [1] studied experimentally the diffusion of ultra-cold ⁸⁷Rb atoms in a one dimensional optical lattice. Starting with a very narrow atomic cloud they recorded the time evolution of the density of the particles, here denoted $P(x, t)$ (normalized to unity). Their work employed the well-known Sisyphus cooling scheme [2]. As predicted theoretically by Marksteiner, et al. [3], the diffusion of the atoms was not Gaussian, so that the assumption that the diffusion process obeys the standard central limit theorem is not valid in this case. An open challenge is to determine the precise nature of the non-equilibrium spreading of the atoms, in particular the dynamical phase diagram of the various different types of behaviors exhibited as the depth of the optical potential is varied. In [1] the anomalous diffusion data was compared to the set of solutions of the fractional diffusion equation [4–6]

$$\frac{\partial^\beta P(x, t)}{\partial t^\beta} = K_\nu \nabla^\nu P(x, t), \quad (1)$$

with $\beta = 1$, so that the time derivative on the left hand side is a first-order derivative. The fractional space derivative on the right hand side is a Weyl-Riesz fractional derivative [6]. Here the anomalous diffusion coefficient K_ν has units cm^ν/sec . A fundamental challenge is to derive fractional equations from a microscopic theory, without invoking power-law statistics in the first place. Furthermore, the solutions of such equations exhibits diverging mean-square displacement $\langle x^2 \rangle = \infty$, which violates the principle of causality [7], which permits physical phenomena to spread at finite speeds. So how can fractional equations like Eq. (1) describe physical reality? We will address this paradox in this work.

The solution of Eq. (1) for an initial narrow cloud is given in terms of a Lévy distributions (see details below). The Lévy distribution generalizes the Gaussian distribution in the mathematical problem of the sum of a large number of independent random variables, in the case where the variance of summands diverges, physically corresponding to scale free systems. Lévy statistics and fractional kinetic equations have found several applica-

tions [6, 8–15], including in the context of sub-recoil laser cooling [16]. Here our aim is to derive Lévy statistics and the fractional diffusion equation from the semi-classical picture of Sisyphus cooling. Specifically we will show that $\beta = 1$ and relate the value of the exponent ν to the depth of the optical lattice U_0 , deriving an expression for the constant K_ν . Furthermore, we discuss the limitations of the fractional framework, and show that for a critical value of the depth of the optical lattice, the dynamics switches to a non-Lévy behavior (i.e. a regime where Eq. (1) is not valid); instead it is related to Richardson-Obukhov diffusion found in turbulence. Thus the semiclassical picture predicts a rich phase diagram for the atomistic diffusion process. We will then compare the results of this analysis to the experimental findings, and see that there are still unresolved discrepancies between the experiment and the theory. Reconciling the two thus poses a major challenge for the future.

Model and goal. In this article we investigate the spatial density of the atoms, $P(x, t)$. The trajectory of a single particle is $x(t) = \int_0^t p(t) dt/m$ where $p(t)$ is its momentum. Within the standard semiclassical picture [2, 3] of Sisyphus cooling, two competing mechanisms describe the dynamics. The cooling force $F(p) = -\bar{\alpha}p/[1 + (p/p_c)^2]$ acts to restore the momentum to the minimum energy state $p = 0$. Momentum diffusion is governed by a diffusion coefficient which is momentum dependent, $D(p) = D_1 + D_2/[1 + (p/p_c)^2]$. The latter describes momentum fluctuations which lead to heating (due to random emission events). We use dimensionless units, time $t \rightarrow t\bar{\alpha}$, momentum $p \rightarrow p/p_c$, the momentum diffusion constant $D = D_1/(p_c)^2\bar{\alpha}$ and $x \rightarrow xm\bar{\alpha}/p_c$. For simplicity, we set $D_2 = 0$ since it does not modify the asymptotic $|p| \rightarrow \infty$ behavior of the diffusive heating term, nor that of the force and therefore does not modify our main conclusions. The Langevin equations

$$\frac{dp}{dt} = F(p) + \sqrt{2D}\xi(t), \quad \frac{dx}{dt} = p \quad (2)$$

describe the dynamics in phase space. Here the noise term is Gaussian, has zero mean and is white $\langle \xi(t)\xi(t') \rangle =$

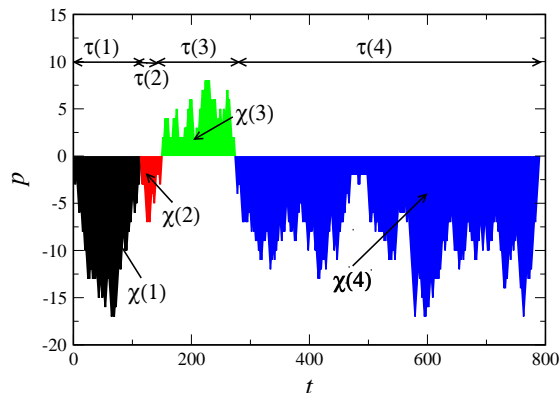


FIG. 1. Schematic presentation of momentum of the particle versus time. The times between consecutive zero crossings are called the jump durations τ and the shaded area under each excursion are the random flight displacements χ . The τ 's and the χ 's are correlated, since statistically a long jump duration implies a large displacement.

$\delta(t - t')$. The now dimensionless cooling force is

$$F(p) = -\frac{p}{1 + p^2}. \quad (3)$$

The stochastic Eq. (2) gives the trajectories of the standard Kramers picture for the semi-classical dynamics in the optical lattice which in turn was derived from microscopical considerations [2, 3]. From the semiclassical treatment of the interaction of the atoms with the counter-propagating laser beams, we have $D = cE_R/U_0$, where U_0 is the depth of the optical potential and E_R the recoil energy, and the dimensionless parameter c [17] depends on the atomic transition involved [2, 3, 18]. For $p \ll 1$, the cooling force Eq. (3) is harmonic, $F(p) \sim -p$, while in the opposite limit, $p \gg 1$, $F(p) \sim -1/p$. The effective potential $V(p) = -\int_0^p F(p)dp = (1/2)\ln(1+p^2)$ is asymptotically logarithmic, $V(p) \sim \ln(p)$ when p is large. This large p behavior of $V(p)$ is responsible for several unusual equilibrium and non-equilibrium properties of the momentum distribution [19–22] while the new experiment [1] demands a theory for the spatial spreading.

The heart of our analysis is the mapping of the Langevin dynamics to a recurrent set of random walks. The particle along its stochastic path in momentum space crosses $p = 0$ many times when the measurement time is long. Let $\tau > 0$ be the random time between one crossing event to the next crossing event, and let $-\infty < \chi < \infty$ be the random displacement (for the corresponding τ). As schematically shown in Fig. 1, the process starting at the origin with zero momentum is defined by the sequence of

jump durations, $\{\tau(1), \tau(2), \dots\}$ with corresponding displacements $\{\chi(1), \chi(2), \dots\}$, with $\chi(1) \equiv \int_0^{\tau(1)} p(\tau)d\tau$, $\chi(2) \equiv \int_{\tau(1)}^{\tau(1)+\tau(2)} p(\tau)d\tau$, etc. The total displacement x at time t is a sum of the individual displacements $\chi(i)$. Since the underlying Langevin process is continuous, we need a more precise definition of this process. We define τ as the time it takes the particle with initial momentum p_i to reach $p_f = 0$ for the first time, where eventually we take $p_i \rightarrow p_f$. Similarly, χ is the displacement of the particle during this flight. The probability density function (PDF) of the displacement χ is denoted $q(\chi)$ and of the jump durations $g(\tau)$.

As shown by Marksteiner, et al. [3], these PDFs exhibit power law behavior

$$g(\tau) \propto \tau^{-\frac{3}{2}-\frac{1}{2D}}, \quad q(\chi) \propto |\chi|^{-\frac{4}{3}-\frac{1}{3D}}, \quad (4)$$

as a consequence of the logarithmic potential, which makes the diffusion for large enough p only weakly bounded. It is this power-law behavior, with its divergent second moment of the displacement χ for $D > 1/5$, which gives rise to the anomalous statistics for x . Importantly, and previously overlooked, there is a strong correlation between the jump duration τ and the spatial extent of the jumps χ . These correlations have important consequences, including the finiteness of the moments of $P(x, t)$ and the $D > 1$ dynamical phase we obtain below. These correlations are responsible, in particular, for the finiteness of the moments of $P(x, t)$. Physically, such a correlation is obvious, since long jump durations involve large momenta, which in turn induce a large spatial displacement. The theoretical development starts then from the quantity $\psi(\chi, \tau)$, the joint probability density of χ and τ . From this, we construct a Lévy walk scheme [23–25] which relates the microscopic information $\psi(\chi, \tau)$ to the atomic packet $P(x, t)$ for large x and t .

Scaling theory for anomalous diffusion. We rewrite the joint PDF $\psi(\chi, \tau) = g(\tau)p(\chi|\tau)$, where $p(\chi|\tau)$ is the conditional probability to find a jump length of χ for a given jump duration τ . Numerically, as shown in Fig. 2, we observed that the conditional probability scales at large times like

$$p(\chi|\tau) \sim \tau^{-\gamma} B(\chi/\tau^\gamma) \quad (5)$$

and $\gamma = 3/2$ and $B(\cdot)$ is a scaling function. To analytically obtain the scaling exponent $\gamma = 3/2$ note that $q(\chi) = \int_0^\infty d\tau \psi(\chi, \tau)$, giving

$$q(\chi) \sim \int_{\tau_0}^\infty d\tau \tau^{-\frac{3}{2}-\frac{1}{2D}} \tau^{-\gamma} B\left(\frac{\chi}{\tau^\gamma}\right) \propto |\chi|^{-\left(1+\frac{1+1/D}{2\gamma}\right)}. \quad (6)$$

Here τ_0 is a time scale after which the long time limit in Eq. (4) holds and is irrelevant for large χ . Comparing Eq. (6) to the second of Eqs. (4) yields the consistency condition $1 + (1 + 1/D)/(2\gamma) = 4/3 + 1/(3D)$ and hence $\gamma = 3/2$, as we observe in Fig. 2.

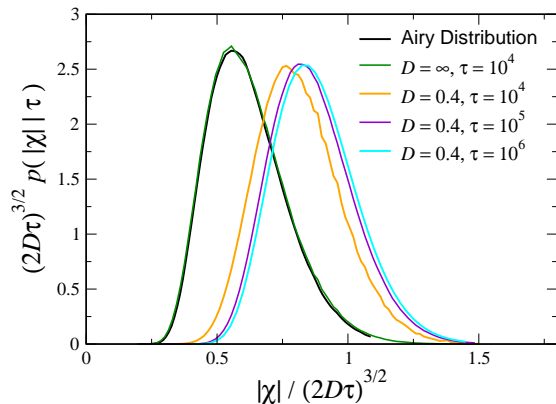


FIG. 2. The scaled conditional probability $(2D\tau)^{3/2}p(|\chi| | \tau)$ versus $|\chi|/(2D\tau)^{3/2}$ for $\tau = 10^4, 10^5$, and 10^6 , for the case $D = 0.4$, from simulations, showing the convergence to an asymptotic scaling form. Also shown is the $D \rightarrow \infty$ limit for $\tau = 10^4$, as well as the analytic result for $\tau \rightarrow \infty$, the Airy distribution [29, 30].

It is interesting to note that $p(\chi|\tau)$ in the case of free diffusion (corresponding to the limit $D \rightarrow \infty$) has been previously considered by mathematicians [26–28] and shown to obey the scaling relation Eq. (5), with B given by the so-called Airy distribution [29, 30]. In the case of finite D , an analytic formula for $p(\chi|\tau)$ can be constructed using the Feynman-Kac formalism [31], giving for asymptotically long walks both $\gamma = 3/2$ and a closed form expression for the scaling function $B(\cdot)$. For our current purposes, however, we do not need the exact form of B ; what is important is the scaling behavior, and the fact that, B falls off rapidly for large argument, ensuring finite moments of this function.

Given our scaling solution for $p(\chi|t)$, and hence $\psi(\chi, t)$, the next step is to construct a theory for the spreading of the particle packet using tools developed in the random walk community [23–25]. One first obtains [31] a Montroll-Weiss [6] type of equation for the Fourier-Laplace transform of $P(x, t)$, $\tilde{P}(k, u)$, in terms of $\tilde{\psi}(k, u)$, the Fourier-Laplace transform of the joint PDF $\psi(\chi, \tau)$:

$$\tilde{P}(k, u) = \frac{\Psi(k, u)}{1 - \tilde{\psi}(k, u)}. \quad (7)$$

Here, $\Psi(k, u)$ is the Fourier-Laplace transform of $\tau^{-3/2}B(|\chi|/\tau^{3/2})[1 - \int_0^t \psi(\tau)d\tau]$. The last step is then to invert Eq. (7) back to the x, t domain.

We now explain why Lévy statistics describes the diffusion profile $P(x, t)$ when $1/5 < D < 1$, provided that x is not too large. The key idea is that, for x 's which are large, but not extremely large, the problem decouples,

and $\tilde{\psi}(k, u)$ can be expressed as a product of the Fourier transform of $q(\chi)$, $\tilde{q}(k)$ and the Laplace transform of $g(\tau)$, $\tilde{g}(u)$. This is valid as long as $x \ll t^{3/2}$, since otherwise paths where $\chi \sim t^{3/2}$ are relevant, for which the correlations are strong, as we have seen. The long-time, large- x behavior of $P(x, t)$ in the decoupled regime is then governed by the small- k behavior of $\tilde{q}(k)$ and the small u behavior of $\tilde{g}(u)$. When the second moment of $q(\chi)$ diverges, i.e. for $D > 1/5$, the small- k behavior of $\tilde{q}(k)$ is determined by the large- χ asymptotics of $q(\chi)$ as given in Eq. (5), $q(\chi) \sim x_*^\nu/|\chi|^{1+\nu}$, where we have introduced the parameter

$$\nu \equiv \frac{1+D}{3D}. \quad (8)$$

When the first moment of τ is finite, i.e. for $D < 1$, the small- u behavior of $\tilde{g}(u)$ is determined by the first moment, $\langle \tau \rangle$: $\tilde{g}(u) \sim 1 - u\langle \tau \rangle$. From these follow the small- k , small- u behavior of $\tilde{P}(k, u)$:

$$\tilde{P}(k, u) \sim \frac{1}{u + K_\nu |k|^\nu} \quad (9)$$

where $K_\nu = \pi x_*^\nu / (\langle \tau \rangle \Gamma(1 + \nu) \sin(\frac{\pi\nu}{2}))$. Both x_*^ν and $\langle \tau \rangle$ can be calculated via appropriate backward Fokker-Planck equations. They both vanish as the magnitude of the initial momentum of the walk goes to zero, but their ratio has a finite limit, so that K_ν , upon returning to dimensionfull units, is

$$K_\nu = \frac{\sqrt{\pi}(3\nu - 1)^{\nu-1} \Gamma(\frac{3\nu-1}{2})}{\Gamma(\frac{3\nu-2}{2}) 3^{2\nu-1} [\Gamma(\nu)]^2 \sin(\frac{\pi\nu}{2})} \left(\frac{p_c}{m}\right)^\nu (\bar{\alpha})^{-\nu+1}. \quad (10)$$

$\tilde{P}(k, u)$, as given in Eq. (9), is in fact precisely the symmetric Lévy distribution in Laplace-Fourier space with index ν , whose (x, t) representation is (see Eq. (B17) of [8])

$$P(x, t) \sim \frac{1}{(K_\nu t)^{1/\nu}} L_{\nu,0} \left[\frac{x}{(K_\nu t^{1/\nu})} \right] \quad (11)$$

It is easy to see that this distribution is the solution of the fractional diffusion equation, Eq. (1), with $\beta = 1$ and an initial distribution located at the origin. This justifies the use of Eq. (1) in Ref. [1] for $1/5 < D < 1$ and provides ν and K_ν in terms of the experimental parameters. We can verify this behavior in simulations, as shown in the upper panel of Fig. 3, where we see excellent agreement to our theoretical prediction, Eqs. (11) and (10), without any fitting.

The lower panel of Fig. 3 illustrates the cutoff on the Lévy distribution, which is found at distances $x \sim t^{3/2}$. Beyond this length scale, the density falls off rapidly. This, as noted above, is the result of the correlation between χ and τ , as there are essentially no walks with a displacement greater than the order of

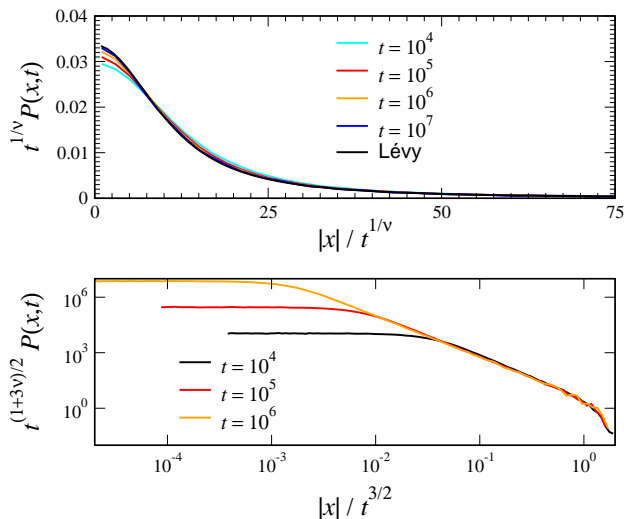


FIG. 3. Upper panel: $t^{1/\nu} P(|x|, t)$ versus $|x|/t^{1/\nu}$ for $D = 2/5$, i.e. $\nu = 7/6$. The theory: Lévy PDF Eq. (11) with K_ν Eq. (10), perfectly matches simulations without fitting. Lower panel: $t^{(1+3\nu)/2} P(|x|, t)$ versus $|x|/t^{3/2}$ for $D = 2/5$, showing the universal crossover from power-law to Gaussian behavior at $|x| \sim t^{3/2}$

$t^{3/2}$. This cutoff ensures the finiteness of the mean square displacement, using the power law tail of the Lévy PDF $L_\nu(x) \sim x^{-(1+\nu)}$ and the cutoff we get: $\langle x^2 \rangle \simeq \int_0^{t^{3/2}} t^{-(1/\nu)} (x/t^{1/\nu})^{-(1+\nu)} x^2 dx \sim t^{4-3\nu/2}$, for $2/3 < \nu < 2$, in agreement with [32]. As noted in the introduction, if we rely on the fractional diffusion equation, Eq. (1), naively, we get $\langle x^2 \rangle = \infty$. Thus the fractional equation must be used with care, realizing its limitations in the statistical description of the moments of the distribution and its tails. When $D < 1/5$, the diffusion is normal since the variance of the walk displacement is finite.

The Obukhov-Richardson phase, $D > 1$. When the average jump duration, $\langle \tau \rangle$, diverges, i.e., for $D > 1$, the dynamics of $P(x, t)$ enters a new phase. Since the Lévy index ν approaches $2/3$ as D approaches 1, x scales like $t^{3/2}$ in the limit. Due to the correlations, x cannot grow faster than this, so in this regime, $P(x, t) \sim t^{-3/2} h(x/t^{3/2})$, which clearly describes a correlated phase. This scaling is that of free diffusion, namely momentum diffuses like $p \sim t^{1/2}$ and hence the time integral over the momentum scales like $x \sim t^{3/2}$. Indeed, in the absence of the logarithmic potential, namely in the limit $D \gg 1$ Eq. (2) gives

$$P(x, t) \sim \sqrt{\frac{3}{4\pi Dt^3}} \exp\left[-\frac{3x^2}{4Dt^3}\right]. \quad (12)$$

This limit describes the Obukhov model for a tracer particle path in turbulence, where the velocity follows a simple Brownian motion [33, 34]. These scaling properties

are related to Kolmogorov's theory of 1941 (see Eq. (3) in [34]) and to Richardson's diffusion $\langle x^2 \rangle \sim t^3$ [32, 35]. Eq. (12) is valid when the optical potential depth is small since $D \rightarrow \infty$ when $U_0 \rightarrow 0$. This limit should be taken with care, as the observation time must be made large before considering the limit of weak potential. In the opposite scenario, i.e. $U_0 \rightarrow 0$ before $t \rightarrow \infty$, we expect ballistic motion, $|x| \sim t$, since then the optical lattice has not had time to make itself felt [1].

The relation to Brownian excursions. Our work shows a surprising connection between the dynamics of cold atoms to the problem of the area under a Brownian excursion [26–30], constrained random walks that start at the origin and return there for the *first* time after t steps. This non-trivial problem has applications in computer science and graph theory and recently to the properties of fluctuating interfaces [29, 30]. Here it corresponds to the calculation of $p(\chi|\tau)$ for the case of $D \rightarrow \infty$ corresponding to free diffusion, since χ is the area under the random walk path in a single excursion (see Fig. 1). The current problem with finite D constitutes an interesting generalization of the problem to logarithmically biased random walks, which has the same scaling exponent but a D -dependent distribution, which in analogy with the term Brownian excursion, we entitle a Bessel excursion. The term Bessel excursion stems from the fact that mathematically speaking, diffusion in momentum space in a non-regularized potential $\ln(p)$ corresponds to a process called the Bessel process [36, 37]. A Bessel excursion is the Langevin path $p(t')$ over the time interval $0 \leq t' \leq \tau$ such that the path starts on $p_0 \rightarrow 0$ and ends on the origin, but is *constrained* to stay positive (if $p_i > 0$) or negative (if $p_i < 0$). In [31] we will provide a detailed account on these constrained random paths.

Discussion of the experiment and summary. Our work shows a rich phase diagram of the dynamics, with two transition points. For deep wells, $D < 1/5$, the diffusion is Gaussian, while for $1/5 < D < 1$ we have Lévy statistics, and for $D > 1$ Richardson-Obukhov scaling, $x \sim t^{3/2}$, is found. We have shown that the correlations between jump durations τ and displacements χ are crucial for the behavior of the tails of the distribution of the total displacement x and are responsible for the finiteness of its second moment. When $D > 1$ the correlations become strong, leading to a breakdown of decoupled Lévy diffusion. So far, experiments have not detected these transitions, though [1] clearly demonstrated that the change in optical potential depth, controls the anomalous exponents in the Lévy spreading packet. In particular so far the experiment showed at most ballistic behavior, with the spreading exponent δ , defined by $x \sim t^\delta$, always less than unity. This might be related to our observation that to go beyond ballistic motion, $\delta > 1$, one must take the measurement time to be very long. A more serious problem is that, in the experimental fitting of the diffusion front to the Lévy propagator,

an additional exponent was introduced [1] to describe the time dependence of the full width at half maximum. In contrast, our semi-classical theory shows that a single exponent ν is needed within the Lévy scaling regime $1/5 < D < 1$, with the spreading exponent $\delta = 1/\nu$. This might be related to the cutoff of the tails of Lévy PDF which demands that the fitting be performed in the central part of the atomic cloud. On the other hand we cannot rule out other physical effects not included in the semiclassical model. For example it would be very interesting to simulate the system with quantum Monte Carlo simulations, though we note that these are not trivial in the $|x| \sim t^{3/2}$ regime since the usual simulation procedure introduces a cutoff on momentum, which may give rise to an artificial ballistic motion. Thus while there is some tantalizing points of contact between the theory and experiment, achieving full agreement will require more study.

This work was supported by the Israel Science Foundation. We thank A. Dechant, E. Lutz, Y. Sagi and N. Davidson for discussions.

-
- [1] Y. Sagi, M. Brook, I. Almog, and N. Davidson, [arxiv:1109.1503v1\[quant-ph\]](#) (2011).
- [2] Y. Castin, J. Dalibard, and C. Cohen-Tannoudji, in *Light Induced Kinetic Effects on Atoms, Ions and Molecules*, edited by L. Moi, S. Gozzini, C. Gabbanini, E. Arimondo, and F. Strumia (ETS Editrice, Pisa, 1991).
- [3] S. Marksteiner, K. Ellinger, and P. Zoller, *Phys. Rev. A* **53**, 3409 (1996).
- [4] A. I. Saichev and G. M. Zaslavsky, *Chaos* **7**, 753 (1997).
- [5] R. Metzler, E. Barkai, and J. Klafter, *Europhys. Lett.* **46**, 431 (1999).
- [6] R. Metzler and J. Klafter, *Phys. Rep.* **339**, 1 (2000).
- [7] See the discussion in Ref. [10] where the unphysical nature of Lévy flights is discussed and the resolution in terms of Lévy walks is addressed.
- [8] J. P. Bouchaud and A. Georges, *Phys. Rep.* **195**, 127 (1990).
- [9] M. F. Shlesinger, G. M. Zaslavsky, and J. Klafter, *Nature* **363**, 31 (1993).
- [10] J. Klafter, M. F. Shlesinger, and G. Zumofen, *Physics Today* **49**, 33 (1996).
- [11] G. M. Viswanathan, S. V. Buldyrev, S. Havlin, M. G. E. da Luz, E. P. Raposo, and H. E. Stanley, *Nature* **401**, 911 (1999).
- [12] E. Barkai, A. V. Naumov, Y. G. Vainer, M. Bauer, and L. Kador, *Phys. Rev. Lett.* **91**, 075502 (2003).
- [13] G. Margolin, V. Protasenko, M. Kuno, and E. Barkai, *J. Phys. Chem. B* **110**, 19053 (2006).
- [14] P. Barthélemy, J. Bartolotti, and D. S. Wiersma, *Nature* **453**, 495 (2008).
- [15] N. E. Humphries, N. Queiroz, J. R. M. Dyer, N. G. Pade, M. K. Musyl, K. M. Schaeferand, D. W. Fuller, J. M. Brunnschweiler, T. K. Doyle, J. D. R. Houghton, G. C. Hays, C. S. Jones, L. R. Noble, V. J. Wearmouth, E. J. Southall, and D. W. Sims, *Nature* **465**, 1066 (2010).
- [16] F. Bardou, J. P. Bouchaud, A. Aspect, and C. Cohen-Tannoudji, *Lévy Statistics and Laser Cooling* (Cambridge Univ. Press, Cambridge, 2002).
- [17] For atoms in molasses with a $J_g = 1/2 \rightarrow J_e = 3/2$ Zeeman substructure in a $\text{lin} \perp \text{lin}$ laser configuration $c = 12.3$ [3]. Refs. [2, 18, 20] give $c = 22$. As pointed out in [3] different notations are used in the literature.
- [18] E. Lutz, *Phys. Rev. Lett.* **93**, 190602 (2004).
- [19] H. Katori, S. Schlipf, and H. Walther, *Phys. Rev. Lett.* **79**, 2221 (1997).
- [20] P. Douglas, S. Bergamini, and F. Renzoni, *Phys. Rev. Lett.* **96**, 110601 (2006).
- [21] D. A. Kessler and E. Barkai, *Phys. Rev. Lett.* **105**, 120602 (2010).
- [22] O. Hirschberg, D. Mukamel, and G. M. Schütz, *Phys. Rev. E* **84**, 041111 (2011).
- [23] J. Klafter, A. Blumen, and M. F. Shlesinger, *Phys. Rev. A* **35**, 3081 (1987).
- [24] A. Blumen, G. Zumofen, and J. Klafter, *Phys. Rev. A* **40**, 3964 (1989).
- [25] E. Barkai and J. Klafter, in *Chaos, Kinetics and Non-linear Dynamics in Fluids and Plasmas: Proceedings of a workshop held in Carry-Le Rouet, France 16-21 June 1997*, Lecture Notes in Physics, Vol. 511, edited by S. Benkadda and G. M. Zaslavsky (Springer, Berlin, 1998) pp. 373–394.
- [26] D. A. Darling, *Ann. Probab.* **11**, 803 (1983).
- [27] G. Louchard, *J. Appl. Probab.* **21**, 479 (1984).
- [28] L. Takacs, *Adv. Appl. Probab.* **23**, 557 (1991).
- [29] S. N. Majumdar and A. Comtet, *Phys. Rev. Lett.* **92**, 225501 (2004).
- [30] S. N. Majumdar and A. Comtet, *J. Stat. Phys.* **119**, 777 (2005).
- [31] D. A. Kessler and E. Barkai, (in preparation).
- [32] A. Dechant, E. Lutz, D. A. Kessler, and E. Barkai, *Phys. Rev. Lett.* **107**, 240603 (2011).
- [33] A. M. Obukhov, *Adv. Geophys.* **6**, 113 (1959).
- [34] A. Baule and R. Friedrich, *Phys. Lett. A* **350**, 167 (2006).
- [35] L. F. Richardson, *Proc. Roy. Soc. Lond. A* **110**, 709 (1926).
- [36] A. J. Bray, *Phys. Rev. E* **62**, 103 (2000).
- [37] G. Schehr and P. Le Doussal, *J. Stat. Mech.: Theory and Expts.* **2010**, P01009 (2010).